JOURNAL OF VIROLOGY, July 1991, p. 3779–3788
0022-538X/91/073779-10$02.00/0

Vol. 65, No. 7

Biochemical Characterization of Epstein-Barr Virus Nuclear Antigen 2A

FRIEDRICH A. GRÄSSER, PETER HAISS, SUSANNE GÖTTEL, AND NIKOLAUS MUELLER-LANTZSCH*

Abteilung Virologie, Institut für medizinische Mikrobiologie und Hygiene, Haus 47, Universitätskliniken des Saarlandes, D-6650 Homburg, Germany

Received 31 December 1990/Accepted 11 April 1991

The Epstein-Barr virus nuclear antigen 2A (EBNA-2A) was immunoprecipitated from latently Epstein-Barr virus-infected lymphocytes with a polyclonal serum raised against the EBNA-2A C terminus. The nucleus contained three subfractions of EBNA-2A which could be distinguished by their resistance to salt extraction: (i) a nucleoplasmatic fraction that was solubilized at 50 mM NaCl, (ii) a chromatin-associated fraction extractable at 1.5 M NaCl, and (iii) a nuclear matrix-associated fraction solubilized only by boiling with buffer containing 2% sodium dodecyl sulfate. The three subfractions were phosphorylated; it was demonstrated that the nucleoplasmatic and the chromatin-associated fractions were phosphorylated at serine and threonine residues. The half-life of the EBNA-2A protein was determined by cycloheximide treatment and by pulse-chase experiments and was found to be at least 24 h. The turnover of the phosphate residues bound to the two salt-soluble subfractions was determined to be approximately 6 to 9 h, suggesting a possible role of the phosphorylation in the regulation of the biological activity of EBNA-2A. Dephosphorylation of EBNA-2A resulted in an increased mobility of the protein during sodium dodecyl sulfate-polyacrylamide gel electrophoresis and indicated the presence of differentially phosphorylated subclasses of the protein. Analysis of EBNA-2A by sucrose gradient centrifugation revealed the existence of two subclasses of complexed molecules which exhibited sedimentation coefficients of approximately 13S and 34S.

Epstein-Barr virus (EBV) is the causative agent of infectious mononucleosis and is tightly associated with two human tumors, Burkitt's lymphoma, and nasopharyngeal carcinoma (for a review, see references 10 and 28). More recently, the presence of viral DNA in about 30 to 60% of all cases of Hodgkin's desease was reported (18). The EBV-encoded nuclear antigen (EBNA) complex is expressed in Burkitt's lymphoma, nasopharyngeal carcinoma, and all lymphocytes immortalized by infection with EBV in vitro (6, 21, 44). In addition to the nuclear antigens, two membrane-associated proteins, the latent membrane protein (LMP) and the terminal protein (designated TP1), have been found in latently infected cells (12, 13, 17, 24, 37). The biological activities of some of the proteins of the EBNA complex are unknown. However, functions have been assigned to the proteins encoded by the EBNA-1, EBNA-2A, EBNA-3C, and LMP genes. EBNA-1 does bind to DNA sequences that are thought to be involved in replication and the maintenance of episomal circular EBV DNA (20, 35). Genetic evidence has implicated a role of the EBNA-2A protein in the immortalization of lymphocytes. The P3HR-1 strain of EBV (type 2 virus) carries a deletion of the *Bam*HI WYH regions (3, 8, 34), does not express EBNA-2B because of this deletion, and does not immortalize lymphocytes in vitro. Reconstitution of a complete viral genome by recombination of the P3HR-1 virus with the deleted sequences derived from a type 1 virus yielded direct proof that EBNA-2A is the gene necessary for immortalization. The reacquisition of the EBNA-2A gene rendered the reconstituted virus fully capable of immortalizing lymphocytes (16). Recent evidence suggested that EBNA-2A has the properties of a transcriptional activator. It apparently stimulates the expression of the LMP gene as well as the expression of the c-*fgr* proto-oncogene (22, 49). The transforming activity of LMP has been demonstrated in vitro (27, 45). In addition, EBNA-2A, EBNA-3c, and LMP have been shown to activate certain lymphocyte-specific surface markers like CD21 or CD23 alone or in concert (1, 2, 4, 46, 47).

EBNA-2A is a phosphoprotein with an apparent molecular mass of approximately 85 kDa on denaturing polyacrylamide gels (9, 30, 38, 39). Comparison of the electrophoretic mobility of EBNA-2A expressed in vitro with that of EBNA-2A isolated from EBV-infected cells on sodium dodecyl sulfate (SDS)-polyacrylamide gels suggested that the protein consists of subfractions which might differ by some form of secondary modification like phosphorylation, glycosylation, or acylation (48). EBNA-2A was localized to various compartments of the nucleus like the nucleoplasm, the chromation fraction, and the nuclear matrix (30, 39). So far, the EBNA-2A protein has been only poorly characterized biochemically. In a series of experiments we wanted to address the following questions: (i) which amino acids are phosphorylated, (ii) what is the rate of metabolic turnover of the EBNA-2A protein compared with the turnover rate of the phosphate residues bound to it, (iii) is the nonhomogeneity of EBNA-2A detectable by gel electrophoresis because of phosphorylation, and (iv) does EBNA-2A exist in different forms of oligomerization?

MATERIALS AND METHODS

Cells and tissue culture. The cell lines M-ABA, Raji, P3HR-1, and BL41 have been described elsewhere (5, 19, 25, 33). The cells were maintained in RPMI 1640 medium (Seromed) supplemented with 10% fetal calf serum (Seromed), 1 mM L-glutamine, penicillin (40 IU/ml), streptomycin (50 μg/ml), Moronal (nystatin; 10 IU/ml), and neomycin sulfate (10 μg/ml) and were subcultured routinely once or twice per week. M-ABA and Raji cells contain complete

* Corresponding author.

EBV genomes (subtype A) and express EBNA-2A, while P3HR-1 cells harbor a partially deleted virus (subtype B) which does not express EBNA-2B (3, 34, 39). BL41 is an EBV-negative Burkitt's lymphoma cell line. The C57/SV cell line which expresses simian virus 40 (SV40) large T antigen was kindly supplied by G. Brandner (21a). The C57/SV cells were cultured in Dulbecco modified Eagle medium supplemented with 3% fetal calf serum and antibiotics as described above.

Radioactive labeling and cell extraction. $H_3{}^{32}PO_4$ ($^{32}P_i$), L-[^{35}S]methionine, and L-[U-^{14}C]proline were purchased from New England Nuclear. Radioactive labeling of proteins with $^{32}P_i$ or L-[^{35}S]methionine was carried out by incubating 10^7 cells with 1 mCi of radioactive label in 1 ml of medium deficient in either phosphate or L-methionine that contained 5% fetal calf serum dialyzed against 10 mM Tris-HCl (Sigma) (pH 7.3)–140 mM NaCl or phosphate-buffered saline (PBS), respectively. Labeling with L-[U-^{14}C]proline was done by incubating 6×10^6 cells in 2 ml of proline-deficient medium supplemented with 100 μCi of radioactive label and 5% fetal calf serum dialyzed against PBS. For pulse-chase experiments, the labeling medium was removed after 4 h and the cells were washed three times with complete medium and then incubated for various times in complete medium.

Cell extract was prepared by washing the cells with ice-cold PBS followed by a 3-min incubation of 2.3×10^7 cells per ml of lysis buffer that contained 10 mM Tris-HCl, pH 7.4, 50 mM NaCl, 2.5 mM $MgCl_2$, 1 mM $CaCl_2$, 300 mM sucrose, 10 mM *N*-ethylmaleimide, 1 mM dithiothreitol, 0.5% Triton X-100, 2 μg of aprotinin per ml, and 2 mM phenylmethylsulfonyl fluoride. The lysate was centrifuged (10 min, 8,000 × *g*, 4°C), and the pellet was washed with the same buffer that did not contain detergent. The combined supernatants were designated low-salt or 50 mM NaCl extract. The pellet was suspended in high-salt buffer (radioimmunoprecipitation assay [RIPA] buffer) containing 10 mM Tris-HCl, pH 7.4, 1.5 M NaCl, 0.5% deoxycholic acid, 0.5% Nonidet P-40, 0.1% SDS, 10 mM *N*-ethylmaleimide, 1 mM dithiothreitol, 2 μg of aprotinin per ml, and 2 mM phenylmethylsulfonyl fluoride, sonicated for 10 s to destroy high-molecular-weight DNA, and incubated for 15 min on ice. After centrifugation, the pellet was washed in the same buffer without NaCl. The combined supernatants were designated 1.5 M NaCl or high-salt extract. The final pellet was boiled in SDS-containing gel loading buffer (125 mM Tris-HCl, pH 6.8, 6% SDS, 10% glycerol, 10% β-mercaptoethanol, and 0.01% bromophenol blue) and designated nuclear matrix extract.

Sucrose gradients. High- and low-molecular-weight complexes of EBNA-2A were separated on sucrose gradients essentially as described by Schickedanz et al. (42). Briefly, 3.5×10^7 cells were washed with ice-cold PBS and extracted for 15 min on ice with 0.1 ml of buffer containing 100 mM Tris-HCl, pH 9.0, 100 mM NaCl, 5 mM KCl, 0.5 mM $MgCl_2$, 1 mM $CaCl_2$, and 0.5% Nonidet P-40. Cellular debris was removed by centrifugation (20 min, 4°C, 45,000 × *g*). The supernatant was layered immediately onto 11.6 ml of a 5 to 30% sucrose gradient in buffer containing 10 mM 2-[4-(2-hydroxyethyl)-1-piperazinyl]-ethanesulfonic acid (HEPES; Merck), pH 7.8, 5 mM Na_3PO_4, 5 mM KCl, 0.5 mM $MgCl_2$, and 1 mM dithiothreitol. The gradient was run in a Sorvall SW41 rotor for 6 h at 260,000 × *g* and 4°C. Sixteen fractions were collected, and protein was precipitated at −20°C with a twofold volume of ethanol. One-half of each fraction was analyzed by SDS-polyacrylamide gel electrophoresis (SDS-PAGE) and immunoblotting.

Antibodies and immunoprecipitation. The production of a polyclonal rabbit serum directed against the carboxyl terminus of EBNA-2A that was used throughout this study for the immunoprecipitation and immunoblotting experiments has been described elsewhere (2, 29, 31). For immunoprecipitation of EBNA-2A, cell extract corresponding to 2×10^7 cells was incubated for 2 h with 2 to 5 μl of antiserum and the immunocomplexes were adsorbed to 25 μl of protein A-Sepharose (Pharmacia) and washed with low-salt lysis buffer and RIPA buffer. The immunocomplexes were released from the matrix by boiling in 100 μl of SDS-containing gel buffer. In some cases, EBNA-2A was further purified by 10-fold dilution of the boiled immunocomplexes in RIPA buffer that contained no NaCl followed by a second round of immunoprecipitation. Immunoblotting analysis of EBNA-2A was performed essentially as described previously (2) with Immobilon-P membranes (Millipore). The membranes were incubated with anti-EBNA-2A antiserum at a 1-to-400 dilution in 5% nonfat milk for at least 3 h. The blots were developed by the peroxidase-antiperoxidase system. Briefly, the membranes were incubated with swine anti-rabbit immunoglobulin followed by a soluble complex of horseradish peroxidase coupled to rabbit anti-horseradish peroxidase immunoglobulin (Dako). The use of this procedure in the immunoblotting of membranes that contained complexes of EBNA-2A and rabbit anti-EBNA-2A resulted in the staining of the blotted immunoglobulins in addition to EBNA-2A. The mouse monoclonal antibody PAb 1605 recognizes the extreme carboxyl terminus of SV40 large T antigen (43) and was generously supplied by G. Brandner.

Inhibition of protein synthesis in vivo with cycloheximide. To determine the turnover of the EBNA-2A protein, M-ABA and P3HR-1 cells were treated with cycloheximide as described by Lüscher and Eisenman (26). Approximately 3×10^5 M-ABA cells per ml and 5×10^5 P3HR-1 cells per ml were suspended in fresh medium that contained cycloheximide (Sigma) at 50 μg/ml. Aliquots corresponding to 6×10^6 cells were removed at various times, the pelleted cells were sonicated and boiled in 100 μl of SDS-containing gel buffer, and the equivalent of approximately 7×10^5 cells was analyzed by immunoblotting as described above. As a control, the same extracts were immunoblotted with a polyclonal rabbit serum directed against the p59/62$^{c\text{-}myc}$, the protein product of the c-*myc* proto-oncogene. The anti-*myc* serum was a generous gift of D. Eick (Munich). The analysis of EBNA-2A under reducing or nonreducing conditions was carried out in standard SDS-containing gel buffer that contained either 10% β-mercaptopropanediol (Sigma; reducing conditions) or 1% iodoacetate (Sigma; nonreducing conditions) as described by Frech et al. (13).

Dephosphorylation of EBNA-2A. Dephosphorylation of EBNA-2A with calf intestinal alkaline phosphatase was carried out essentially as described by Grässer et al. (14). The EBNA-2A corresponding to approximately 2×10^7 cells was immunoprecipitated and bound to 25 μl of protein A-Sepharose; washed with alkaline phosphatase buffer that consisted of 20 mM Tris-HCl, pH 8.5, 100 mM NaCl, 5 mM $MgCl_2$, and 2 μg of aprotinin per ml; resuspended in 25 μl of the same buffer; and kept under occasional agitation at 37°C for 30 min after the addition of 1 μl (22 U) of alkaline phosphatase (Boehringer Mannheim; molecular biology grade). The reaction was terminated by the addition of 1 ml of RIPA buffer. Dephosphorylation of EBNA-2A with potato acid phosphatase was performed as described above. The dephosphorylation buffer contained 20 mM (*N*-morpholino)ethylsulfonic acid (MES; Calbiochem), pH 5.5, 100

mM NaCl, 1 mM MgCl, and 2 μg of aprotinin per ml. Potato acid phosphatase (Boehringer) was dialyzed against phosphatase buffer at pH 5.5. Then 25 μl of the beads containing the EBNA-2A immunocomplex was washed with phosphatase buffer and resuspended in 25 μl of the dialyzed enzyme (approximately 33 U/ml). After the dephosphorylation reaction, the reaction products were analyzed by SDS-PAGE and immunoblotting.

Phosphoamino acid analysis of EBNA-2A. Phosphoamino acid analysis of ^{32}P-labeled EBNA-2A was carried out as described elsewhere (15, 36). In vivo ^{32}P-labeled EBNA-2A was immunoprecipitated, subjected to SDS-PAGE, and visualized by autoradiography. The protein was excised from the unfixed, dried gel and eluted with a buffer containing 50 mM $(NH_4)_2CO_3$, 0.1% SDS, and 5% β-mercaptoethanol. After the addition of 10 μg of bovine serum albumin as a carrier, the protein was precipitated by the addition of 10% trichloroacetic acid, washed with 100% ethanol, and hydrolyzed in 100 μl of 6 M HCl for 2 h at 115°C. The reaction products were lyophylized and analyzed by one- or two-dimensional thin-layer chromatography. The reaction products were visualized by autoradiography with intensifying screens. Unlabeled phosphoserine, phosphothreonine, and phosphotyrosine (Sigma) (1 μg each) were included to facilitate the ninhydrin staining (Sigma) of the separated phosphoamino acids.

RESULTS

Immunoprecipitation of EBNA-2A from EBV-infected cells. A polyclonal rabbit serum that was raised against the bacterially expressed carboxyl terminus of EBNA-2A had originally been shown to recognize EBNA-2A in immunoblotting experiments (2). We asked whether this serum could immunoprecipitate EBNA-2A from cell extracts prepared from lymphoid cells infected with EBV. M-ABA cells which harbor a full-length, biologically active EBV genome of the A subtype were metabolically labeled with [^{35}S]methionine and fractionated as described in Materials and Methods. The anti-EBNA-2A serum was used in two consecutive rounds of immunoprecipitation. The immunoprecipitate was analyzed by SDS-PAGE and autoradiography as shown in Fig. 1a. We observed a single band corresponding to EBNA-2A in both the low- and high-salt fractions that were tested (lanes 2 and 4, respectively). The preimmune serum did not precipitate a protein corresponding to EBNA-2A (lanes 1 and 3). A single immunoprecipitation yielded a discernible band of the EBNA-2A protein, although with a high background of unspecifically precipitated proteins (data not shown). Immunoprecipitation of the SDS-soluble pellet designated the nuclear matrix fraction did not yield detectable amounts of EBNA-2A (data not shown). We found that treatment of the cells with buffer containing 50 mM NaCl already released a substantial amount of EBNA-2A compared with the amount released in the following extraction with buffer that contained 1.5 M NaCl in addition to an increased amount of detergent. We wanted to determine whether the nuclear matrix fraction still contained EBNA-2A protein that was not released by high-salt–detergent treatment of the cell extract. The low- and high-salt fractions prepared from M-ABA, Raji, and P3HR-1 cells were subjected to a single round of immunoprecipitation. The immunocomplexes were resolved on a 12.5% SDS-polyacrylamide gel together with the nuclear matrix fraction that was obtained by extraction with SDS-containing gel buffer of the pellet left after the high-salt extraction. The proteins were transferred to an Immobilon membrane and immunoblotted with the anti-EBNA-2A serum. The results of these experiments are shown in Fig. 1b to d. The immunoblot confirmed that the low-salt treatment released a major portion of the soluble fraction of EBNA-2A prepared from M-ABA cells compared with that released by the high-salt treatment (compare lane 2, low-salt fraction, and lane 4, high-salt fraction, in panel b). However, the nuclear matrix fraction also contained a sizable amount of immunoreactive EBNA-2A protein, as can be seen in lane 5. We do not know why only a small portion of the EBNA-2A protein that was solubilized from the nuclear matrix fraction by boiling with SDS-containing buffer could be immunoprecipitated compared with the relatively large amount of EBNA-2A detected in the immu-

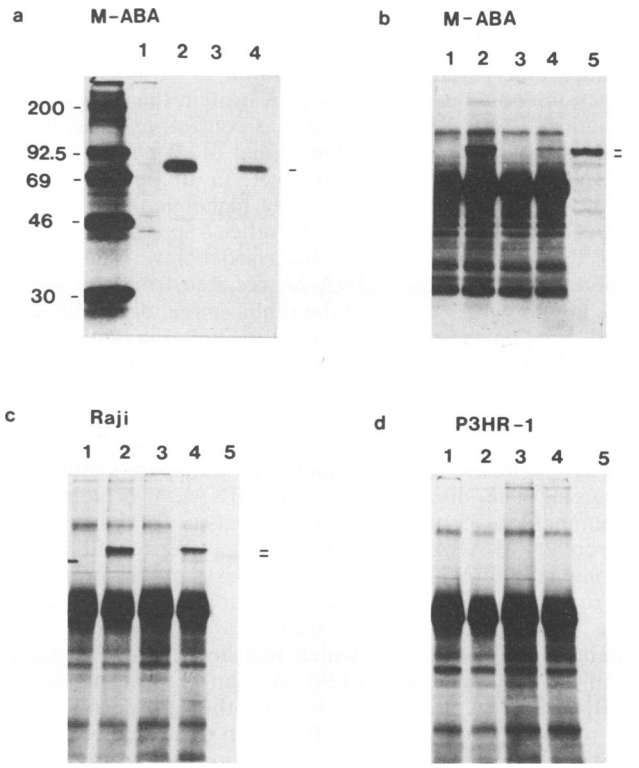

FIG. 1. Immunoprecipitation of EBNA-2A. (a) M-ABA cells were metabolically labeled with [^{35}S]methionine in methionine-deficient medium and fractionated as described in Materials and Methods. The soluble low- and high-salt fractions (lanes 1 and 2 and lanes 3 and 4, respectively) of the cell extract were immunoprecipitated twice with preimmune serum (lanes 1 and 3) or with serum directed against the carboxyl terminus of EBNA-2A (lanes 2 and 4). The reaction products were analyzed on a 12.5% SDS-polyacrylamide gel followed by autoradiography. The molecular masses of the protein markers are indicated on the left in kilodaltons. The horizontal bar on the right indicates the position of EBNA-2A. The ^{14}C-methylated molecular mass markers (Amersham) are as follows: myosin, 200 kDa; phosphorylase b, 92.5 kDa; bovine serum albumin, 68 kDa; ovalbumin, 46 kDa; carbonic anhydrase, 30 kDa. (b, c, and d) M-ABA, Raji, and P3HR-1 cells, respectively, were fractionated and subjected to a single round of immunoprecipitation, gel electrophoresis, and transfer to Immobilon membranes. EBNA-2A was visualized by the peroxidase antiperoxidase staining procedure as described in Materials and Methods. Lanes 1 to 4 are as in panel a; lanes 5 represent the immunoblots of the SDS-solubilized nuclear matrix loaded onto the gels without prior immunoprecipitation. The position of EBNA-2A is indicated by horizontal bars on the right sides of panels b and c.

noblot of the nuclear matrix fraction (Fig. 1b, lane 5). The same treatment of extracts prepared from Raji cells yielded comparable results (panel c), although the nuclear matrix fraction contained less EBNA-2A protein than the high-salt fraction. P3HR-1 cells served as a control; as expected, no EBNA-2A could be detected (panel d). We noted that the EBNA-2A-specific band observed in the nuclear matrix fractions migrated with a slightly higher mobility than the EBNA-2A-specific bands of the other fractions. The reason for this difference will be discussed below. The strongly stained bands below EBNA-2A resulted from the staining technique, which detected the rabbit immunoglobulin heavy and light chains from the immunoprecipitation that were also transferred to the membranes (see Materials and Methods).

Metabolic stability of the EBNA-2A protein. We used two different approaches to determine the metabolic turnover of the EBNA-2A protein. First, we carried out experiments using cycloheximide to block the de novo synthesis of protein. The disappearance of EBNA-2A protein in an immunoblot should then give a measure of its metabolic turnover. M-ABA and P3HR-1 cells were treated with cycloheximide for 32 h, and total-cell extract was prepared at various times and analyzed by immunoblotting. As a control, the same extracts were tested in a parallel blot for the stability of p59/62$^{c\text{-}myc}$, which had been shown to have a half-life of less than 1 h (26). As can be seen in Fig. 2A, EBNA-2A was stable for 32 h, while the band corresponding to p59/62$^{c\text{-}myc}$ disappeared after a 1-h treatment with cycloheximide (panel B). A longer incubation with cycloheximide was not performed, since the exposure of the cells to the chemical eventually leads to cell death. Secondly, a pulse-chase experiment was performed to determine the stability of the EBNA-2A protein in the cell. M-ABA cells were metabolically labeled with [^{14}C]proline for 4 h followed by a 24-h chase period. After cell fractionation, EBNA-2A was immunoprecipitated and analyzed by gel electrophoresis and autoradiography, as shown in Fig. 2C. Again, EBNA-2A was specifically recognized by the immunserum. We did not observe a significant decrease in the intensity of the EBNA-2A signal, indicating that the protein has a half-life of at least 24 h; the high-salt fraction did not yield a signal, probably because the low-salt fraction of EBNA-2A already comprised the major portion of the protein in M-ABA cells that can be precipitated from these cells under the described experimental conditions (data not shown). This result confirmed the observation that the EBNA-2A protein is very stable, with a half-life of at least 24 h.

EBNA-2A is phosphorylated at serine and threonine residues. In order to analyze the phosphorylation of EBNA-2A, M-ABA cells were metabolically labeled with $^{32}P_i$ and cell extracts were subjected to immunoprecipitation. We found that the three subfractions described above yielded a phosphorylated band of EBNA-2A when analyzed by SDS-PAGE and autoradiography. A representative immunoprecipitation is shown in Fig. 3a, which displays the results of an experiment that was carried out to determine the turnover of phosphate residues bound to EBNA-2A. A single band of ^{32}P-labeled EBNA-2A was observed in the immunoprecipitates from the low- and high-salt fractions. Furthermore, a weak band corresponding to EBNA-2A derived from the nuclear matrix fraction could be detected (Fig. 3a, lane NM). The phosphorylated form isolated from the low- and high-salt fractions of M-ABA cells was eluted from the gel, subjected to acid hydrolysis, and analyzed by two-dimensional phosphoamino acid analysis. The result obtained for EBNA-2A from the low-salt fraction is displayed in Fig. 3b.

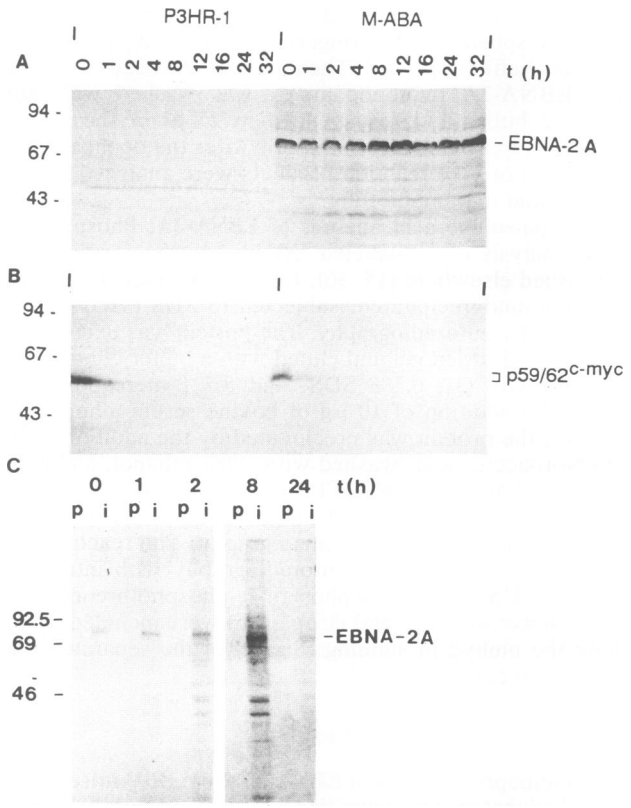

FIG. 2. Metabolic stability of the EBNA-2A protein. (A) P3HR-1 and M-ABA cells were treated with cycloheximide for the indicated times. Total-cell extract was prepared and analyzed by gel electrophoresis and immunoblotting with anti-EBNA-2A serum. (B) The material used in panel A was tested in parallel by immunoblotting with an antiserum directed against p59/62$^{c\text{-}myc}$. The positions of EBNA-2A, p59/62$^{c\text{-}myc}$, and the molecular mass marker proteins are indicated. The molecular mass marker proteins (Pharmacia) are as follows: phosphorylase b, 94 kDa; bovine serum albumin, 67 kDa; ovalbumin, 43 kDa; carbonic anhydrase, 30 kDa. (C) Pulse-chase experiment. M-ABA cells were labeled for 4 h with ^{14}C-proline (pulse), washed, and incubated in complete medium for various lengths of time (chase) as indicated. Cell extract was reacted with preimmune (p) or immune (i) serum and analyzed by SDS-PAGE and autoradiography. The exposure time was 8 weeks. Molecular mass markers were as in Fig. 1a.

We observed that only serine and threonine residues, but no tyrosine residues, were modified. Unlabeled phosphoserine, phosphothreonine, and phosphotyrosine that had been added to the hydrolysate were stained with ninhydrin to ensure that the separation was complete (data not shown). EBNA-2A from the high-salt fraction also contained no phosphotyrosine (data not shown). Comparable results were obtained when EBNA-2A from the pulse-chase experiments described below was subjected to one-dimensional phosphoamino acid analysis (Fig. 3c). Although we cannot rigorously rule out a low level of phosphorylation at tyrosine residues, it appeared that EBNA-2A subfractions isolated after low- and high-salt treatment of the cells did not contain phosphotyrosine. The nuclear matrix fraction did not yield enough ^{32}P-labeled EBNA-2A to perform a phosphoamino acid analysis.

The half-life of phosphate bound to EBNA-2A. In order to determine the metabolic stability of the phosphates bound to

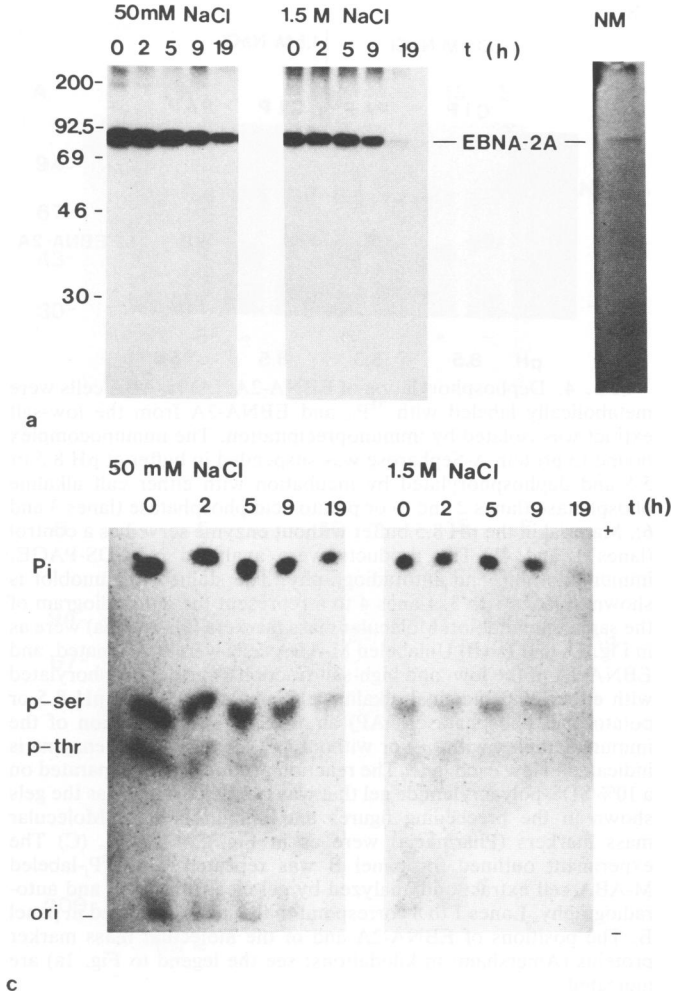

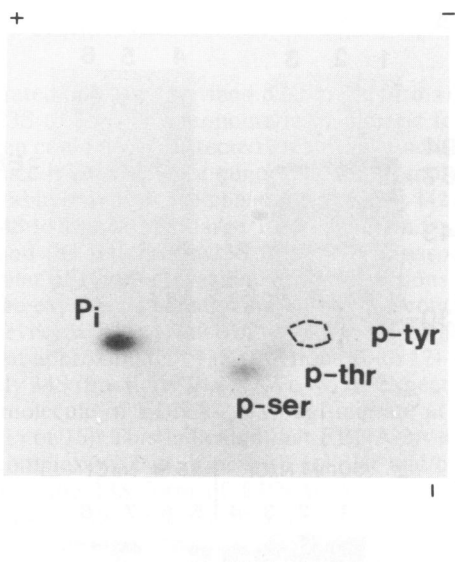

FIG. 3. Metabolic stability of phosphate residues bound to EBNA-2A. (a) M-ABA cells were metabolically labeled with $^{32}P_i$ for 4 h in phosphate-free medium (pulse), washed, and incubated in complete medium (chase). Cell extracts were prepared at the times indicated; EBNA-2A from the low- and high-salt fractions was immunoprecipitated and analyzed by SDS-gel electrophoresis and autoradiography with intensifying screens. In a parallel experiment, EBNA-2A was solubilized from the nuclear matrix of ^{32}P-labeled M-ABA cells by SDS treatment and analyzed as described above. The result is shown in lane NM. The positions of EBNA-2A and of the ^{14}C-methylated molecular mass marker proteins (Amersham; in kilodaltons; see the legend to Fig. 1) are indicated. (b) Two-dimensional phosphoamino acid analysis of EBNA-2A isolated from the low-salt fraction. In vivo $^{32}P_i$-labeled EBNA-2A derived from the low-salt fraction of M-ABA cells was subjected to acid hydrolysis followed by two-dimensional gel electrophoresis and chromatography as described in Materials and Methods. Nonradioactive phosphoamino acids were included in the analysis and visualized by staining with ninhydrin (not shown). The position of phosphotyrosine is indicated by a circle. (c) One-dimensional phosphoamino acid analysis of the EBNA-2A protein shown in panel a. The bands corresponding to EBNA-2A were excised and subjected to acid hydrolysis and chromatography as described in Materials and Methods.

EBNA-2A, pulse-chase experiments were performed. M-ABA cells were metabolically labeled with $^{32}P_i$ for 4 h (pulse), washed repeatedly with PBS, and incubated with complete medium for various amounts of time (chase). The low- and high-salt extracts were immunoprecipitated and analyzed on a 12.5% SDS-polyacrylamide gel. The result shown in Fig. 3a indicated that the half-life of the phosphate residues bound to EBNA-2A was approximately 6 to 9 h. This observation was confirmed when the individual bands corresponding to EBNA-2A were eluted from the gel and counted in a beta counter (data not shown). The eluted protein was subjected to a phosphoamino acid analysis, as shown in Fig. 3c. Again, we observed only phosphorylation of serine and threonine residues. Ninhydrin staining demonstrated that the three different phosphoamino acids had effectively separated even during one-dimensional electrophoresis (data not shown). Because of the small amount of ^{32}P-labeled EBNA-2A that could be isolated from the nuclear matrix, this fraction was not tested for the turnover of ^{32}P bound to EBNA-2A. In addition, we were not sure whether quantitative determinations could be obtained by immunoprecipitations involving SDS-boiled material.

Phosphorylation of EBNA-2A decreases its electrophoretic mobility. A comparison of the different fractions of EBNA-2A displayed in Fig. 1 had already revealed that the protein migrated at different rates (compare, for instance, lanes 4 and 5 in Fig. 1b and c). To test whether this difference was due to phosphorylation, we isolated EBNA-2A from the low-salt extract obtained from ^{32}P-labeled M-ABA cells and treated the immunocomplex either with calf intestinal alkaline phosphatase or with potato acid phosphatase. The reaction products were analyzed by immunoblotting and autoradiography. The result is shown in Fig. 4A. The immunoblot (lanes 1 to 3) demonstrated that the treatment had left EBNA-2A largely intact, although a slight increase in electrophoretic mobility of the dephosphorylated protein could be noticed (lanes 2 and 3). The immunoblot was subsequently exposed to X-ray film, which is shown in the adjacent lanes 4 to 6. One strong signal from the untreated control was observed (lane 4), while the alkaline phosphatase (lane 5) removed a major portion of the radioactive label. The acid phosphatase (lane 6) dephosphorylated EBNA-2A almost completely. The same experiment was performed using both the low- and high-salt fractions from unlabeled cells, but proteins were analyzed by performing the SDS-PAGE for twice the usual time. The result of this

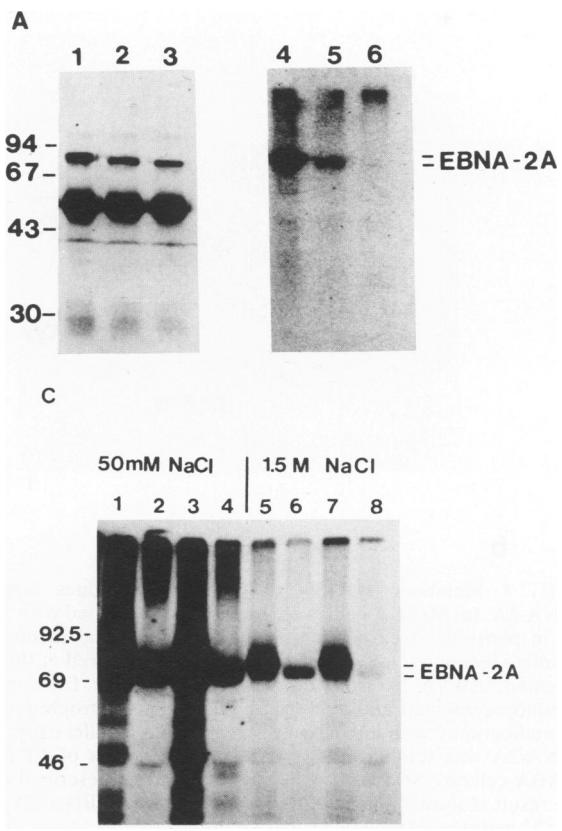

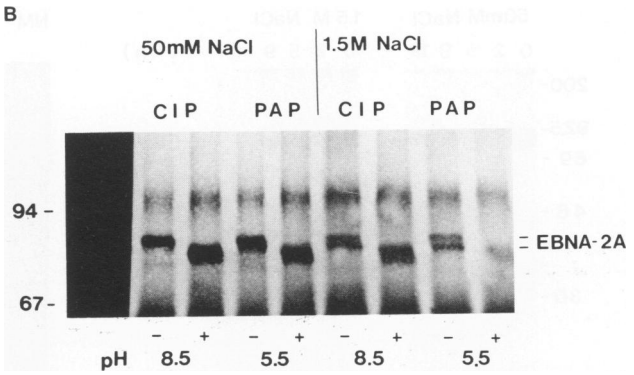

FIG. 4. Dephosphorylation of EBNA-2A. (A) M-ABA cells were metabolically labeled with $^{32}P_i$, and EBNA-2A from the low-salt extract was isolated by immunoprecipitation. The immunocomplex bound to protein A-Sepharose was suspended in buffer at pH 8.5 or 5.5 and dephosphorylated by incubation with either calf alkaline phosphatase (lanes 2 and 5) or potato acid phosphatase (lanes 3 and 6). Material in the pH 8.5 buffer without enzyme served as a control (lanes 1 and 4). The products were analyzed by SDS-PAGE, immunoblotting, and autoradiography. The stained immunoblot is shown in lanes 1 to 3. Lanes 4 to 6 represent the autoradiogram of the same immunoblot. Molecular mass markers (Pharmacia) were as in Fig. 2A and B. (B) Unlabeled M-ABA cells were fractionated, and EBNA-2A of the low- and high-salt fractions was dephosphorylated with either calf intestinal alkaline phosphatase (CIP) at pH 8.5 or potato acid phosphatase (PAP) at pH 5.5. The incubation of the immunocomplex with (+) or without (−) the addition of enzyme is indicated below each lane. The reaction products were separated on a 10% SDS-polyacrylamide gel that was run twice as long as the gels shown in the preceeding figures and immunoblotted. Molecular mass markers (Pharmacia) were as in Fig. 2A and B. (C) The experiment outlined for panel B was repeated with $^{32}P_i$-labeled M-ABA cell extract and analyzed by gel electrophoresis and autoradiography. Lanes 1 to 8 correspond to the lanes displayed in panel B. The positions of EBNA-2A and of the molecular mass marker proteins (Amersham; in kilodaltons; see the legend to Fig. 1a) are indicated.

experiment is shown in Fig. 4B. Again, treatment with either phosphatase resulted in an increase in the electrophoretic mobility of EBNA-2A. To our surprise, we noticed that the untreated EBNA-2A separated into two forms with different mobilities. This was most obvious in the material isolated from the high-salt fraction, although EBNA-2A from the low-salt fraction also appeared to separate into two noticeable bands. In addition, the dephosphorylated EBNA-2A from both the low- and high-salt fractions appeared to migrate slightly ahead of the faster-migrating form of the untreated EBNA-2A. These results indicated that the dephosphorylation and not a fortuitous secondary event like starvation of the cells for phosphorus was responsible for the change in mobility. These experiments were repeated with in vivo-$^{32}P_i$-labeled cell extract, as shown in Fig. 4C. In addition to the major band of untreated EBNA-2A (lanes 1, 3, 5, and 7), a minor species of ^{32}P-labeled material which is barely detectable in the photographic reproduction was detectable by eye underneath the major band. We also observed an increase in mobility when dephosphorylated EBNA-2A protein was compared with the untreated control. In the autoradiogram displayed in Fig. 4C, we still observed a signal from the dephosphorylated protein, indicating that some phosphate remained bound to EBNA-2A (lanes 2, 4, 6, and 8). However, this partially dephosphorylated EBNA-2A migrated with an intermediate mobility compared with that of the two forms of untreated EBNA-2A (compare, for instance, lanes 5 and 6 and lanes 7 and 8 in Fig. 4C). In contrast, the immunoblot shown in panel B indicated that the majority of the dephosphorylated protein migrated faster than the two bands observed with untreated material. Taken together, the data obtained from the immunoblot and the autoradiogram shown indicated that EBNA-2A exists in various states of phosphorylation that influence the mobility of the protein on SDS-polyacrylamide gels. We exclude proteolytic degradation of the phosphatase-treated EBNA-2A, since treatment of SV40 large T antigen under identical conditions did not result in degradation (13a). A graphical determination of the molecular mass of the dephosphorylated and the untreated EBNA-2A revealed that the untreated, slower-migrating form had an apparent molecular mass of approximately 84 kDa, while the dephosphorylated form of EBNA-2A migrated with an apparent molecular mass of approximately 80 kDa (data not shown). These results are in good agreement with the value given by Wang et al. (48).

In M-ABA and in Raji cells, a detectable portion of the EBNA-2A protein was bound to the nuclear matrix (Fig. 1b and c). It appeared that at least a part of these molecules migrated with a higher mobility compared with that of EBNA-2A isolated from the low- and high-salt fractions, even when the proteins were analyzed under normal conditions. In contrast, no size difference was observed when the ^{32}P-labeled proteins were compared (Fig. 3a). It is possible that the majority of EBNA-2A molecules bound to the nuclear matrix existed in a non-low-phosphorylated state, which might exist in a conformation that cannot be bound or can be only poorly bound by our antibody during an immunoprecipitation.

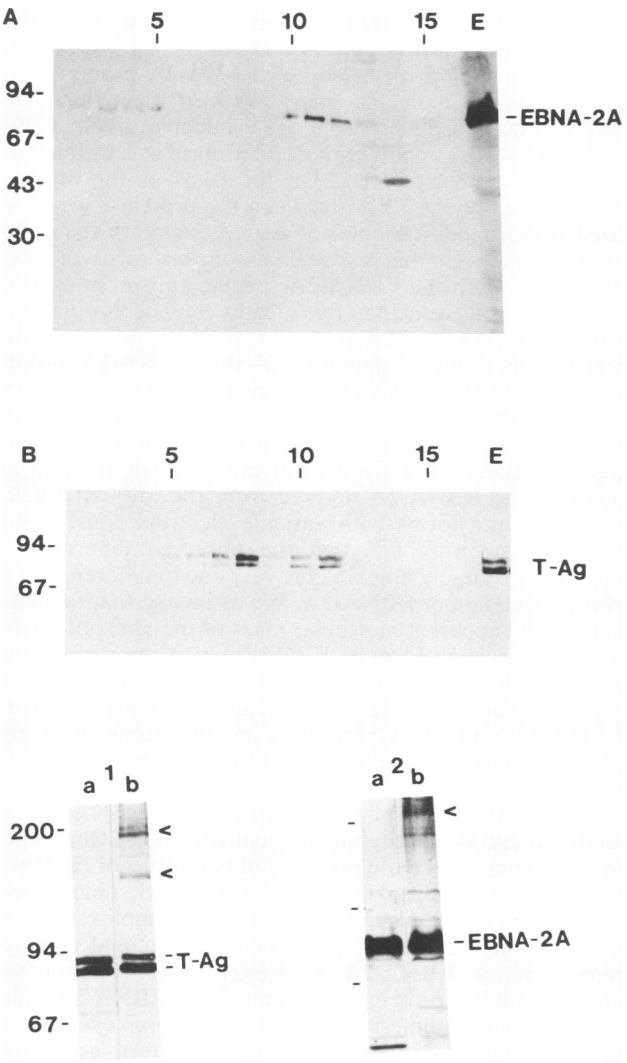

FIG. 5. Oligomerization of EBNA-2A. (A) Whole-cell extract from M-ABA cells was applied to a 5 to 30% sucrose gradient which was run for 6 h at 260,000 × *g*. Sixteen fractions were collected, and protein was ethanol precipitated and separated on a 12.5% SDS-polyacrylamide gel. EBNA-2A was visualized by immunoblotting. (B) Cell extract from C57/SV cells which express high levels of SV40 large T antigen was analyzed as described for panel A for the presence of large T antigen. Lanes E (A and B) contained whole-cell extract. (C) Analysis of SV40 large T antigen and EBNA-2A. Cell extracts of C57/SV cells (panel 1) and M-ABA cells (panel 2) were analyzed by SDS-PAGE under reducing (lanes a) or nonreducing (lanes b) conditions and subsequently immunoblotted. The positions of the major immunoreactive bands of EBNA-2A or SV40 large T antigen and of the molecular mass marker proteins are indicated. Molecular mass marker proteins (GIBCO) were as follows: myosin, 200 kDa; phosphorylase b, 94 kDa; bovine serum albumin, 68 kDa.

Oligomerization of EBNA-2A. To determine the state of oligomerization of EBNA-2A, whole-cell extract from M-ABA cells was prepared according to published procedures and separated on 5 to 30% sucrose gradients (11, 42). The different fractions obtained were precipitated with ethanol and analyzed by gel electrophoresis and immunoblotting, as shown in Fig. 5A. Gradients with cell extract that contained SV40 large T antigen were assayed in parallel and served as a control (Fig. 5B). We found that SV40 large T antigen separated into the described oligomeric forms of 14S to 16S and 23S to 25S. The monomeric or dimeric form of large T antigen could not be detected under the conditions of this assay since it constitutes a minor fraction of molecules that is detectable only in pulse-chase experiments (42). The tetrameric 14S to 16S form of large T was found in fractions 10 and 11, and the tetrameric 23S to 25S form associated with the cellular p53 protein was localized in fractions 5 to 8 (panel B). The experiments analyzing EBNA-2A-containing cell extract revealed the presence of two forms of EBNA-2A sedimenting at approximately 13S (fractions 10 to 12) and at approximately 34S (fractions 3 to 5). We would expect that a monomeric molecule of EBNA-2A would migrate at about 5S (fraction 15 or 16). This indicated that EBNA-2A existed either as a complex with itself or with cellular and/or viral proteins. Since the 13S form of EBNA-2A migrated to a similar position on the gradient as the tetrameric form of large T antigen, one could speculate that this fraction of the EBNA-2A molecules also consisted of tetrameric molecules. It is also conceivable, however, that the 13S form of EBNA-2A represented a monomer or dimer associated with unknown cellular and/or viral proteins. In contrast, the large complex of EBNA-2A migrated further into the gradient than the corresponding fraction of the large T molecules, indicating that it consisted of higher-order complexes than the SV40 large T tetramers that have been described to migrate at 23S. The strongly immunoreactive band at approximately 40 to 50 kDa visible in fraction 14 can also be observed in extracts from P3HR-1 cells (data not shown).

A second approach to analyze the complex formation of EBNA-2A with large T antigen as a control was to separate the proteins on SDS-polyacrylamide gels under reducing and nonreducing conditions. The result of such an experiment is shown in Fig. 5C. While only one band of EBNA-2A that migrated with an apparent molecular mass of 85 kDa was detectable under reducing conditions, additional bands with much lower electrophoretic mobilities could be obtained under nonreducing conditions (Fig. 5C, lane 2b). A high-molecular-weight species of an unspecifically cross-reacting protein or protein complex could also be observed in the control experiment involving P3HR-1 cell extract (data not shown). Similar results were observed with large T antigen, indicating the presence of complexed EBNA-2A molecules.

The immunoblot shown in Fig. 5A also revealed the presence of small amounts of EBNA-2A in fractions 13 to 15 which contained low-molecular-weight forms of protein. It is therefore possible that EBNA-2A also exists in a monomeric or dimeric form as described for SV40 large T antigen.

DISCUSSION

In this report, we describe experiments that were carried out to determine some of the biochemical parameters of EBNA-2A. Specifically, we wished to analyze the metabolic turnover of EBNA-2A and of the phosphate residues bound to it, the nature of the phosphorylated residues, and the state of oligomerization of the EBNA-2A protein. First, we demonstrated that a previously described polyclonal rabbit serum directed against the carboxyl terminus of EBNA-2A immunoprecipitated the protein from extracts of EBV-infected cells. The initial step of the fractionation experiments was based on a procedure that had been shown to separate the unbound from the chromatin-associated fraction of SV40 large T antigen (41). Our experiments revealed three subfractions of EBNA-2A. A soluble form of the protein could be isolated from cell extract prepared at low ionic strength

that included the cytoplasm and the nucleoplasm. A stepwise increase in the salt concentration indicated the existence of a second, chromatin-associated subfraction of EBNA-2A that was released only at 1.5 M NaCl but not at lower ionic strength. Repeated washing with buffer that contained, in addition to 1.5 M NaCl, a larger amount of detergent did not release any more EBNA-2A (data not shown). In addition, we found a third subfraction that was tightly bound to the nuclear matrix and could be released only by boiling with SDS-containing electrophoresis buffer. These results were in accordance with results published by others (30) while this work was in progress. It appeared that the bulk of EBNA-2A existed in a soluble form, while a smaller portion of the protein was bound to the chromatin. In cells infected with the M-ABA strain of EBV, the nuclear matrix-associated fraction of EBNA-2A contained more EBNA-2A protein than the fraction bound to chromatin. In the case of Raji cells, which are also infected with type 1 virus, the nucleoplasmatic fraction again contained more EBNA-2A protein than the chromatin fraction. For unknown reasons, the nuclear matrix of Raji cells contained proportionally less EBNA-2A than the M-ABA nuclear matrix fraction.

We asked whether all three subcellular fractions of EBNA-2A were phosphorylated. This was indeed the case, and we were able to show that the soluble and chromatin-associated forms of EBNA-2A are phosphorylated at serine and threonine residues, but apparently not at tyrosine. The amount of $^{32}P_i$-labeled EBNA-2A that was solubilized from the nuclear matrix and reisolated by immunoprecipitation was too small to be analyzed for its phosphorylated phosphoamino acids. For unknown reasons, only a very small portion of EBNA-2A that was solubilized from the nuclear matrix by boiling in SDS-containing gel buffer could be immunoprecipitated, while EBNA-2A from the other subcellular fractions could be reprecipitated after such a treatment. The higher mobility of matrix-bound EBNA-2A would indicate that this subfraction is un- or underphosphorylated. This could affect the secondary structure of the protein to render the C terminus inaccessible to the antibody.

In the case of SV40 large T antigen, phosphorylation had been shown to regulate some of its biochemical properties (for a review, see reference 32). The phosphorylation appeared to be reversible, and it was suggested that phosphorylation-dephosphorylation might serve to functionally "recycle" SV40 large T antigen from a less active, phosphorylated form to an active, underphosphorylated form (40). A high turnover of the phosphate residues compared with that of the protein itself should therefore be a prerequisite for such a process. When we analyzed EBNA-2A, we also found that the turnover of the phosphate residues, which we estimated at 6 to 9 h, was much higher than the turnover of the EBNA-2A protein, which appeared to be at least 24 h or longer. The values given above are only rough estimates, since we do not know how fast the radioactive label in proteins other than EBNA-2A is recycled to the cellular pool of free amino acids that could be reincorporated into EBNA-2A. Also, the real turnover of phosphate bound to EBNA-2A might be higher, since a large amount of label might be recycled from other phosphate-utilizing proteins or enzymatic reactions involving phosphate. Although we need experimental evidence to prove that phosphorylation serves to modulate the biochemical properties of EBNA-2A, the higher turnover of the phosphates bound to EBNA-2A compared with that of the protein itself might indicate that phosphorylation does influence some of its properties.

In vitro translation-transcription experiments had shown that translation of the naturally occurring EBNA-2A transcription unit in vitro yielded an EBNA-2A protein with a lower apparent molecular mass (80 kDa) than that of the native protein isolated from EBV-infected tissue culture cells (48), whose apparent molecular mass was estimated to be approximately 85 kDa. On the basis of the observed difference of about 5 kDa between the proteins, we speculated that a modification(s) of EBNA-2A other than phosphorylation might be responsible for this relatively large difference. With the EBNA-2A-specific antiserum as a tool at our disposal, we tested this idea by dephosphorylation of EBNA-2A. We could demonstrate that dephosphorylation resulted in a higher mobility of the EBNA-2A protein, regardless of the dephosphorylating enzyme or the subfraction of EBNA-2A used. When the gel electrophoresis was performed twice as long as normally, we noticed that untreated EBNA-2A derived from the high-salt fraction and possibly the EBNA-2A derived from the low-salt fraction separated into forms with variable electrophoretic mobilities. We therefore feel that the observed differences in mobility are largely if not exclusively due to difference in the phosphorylation of EBNA-2A. We estimated that the difference in the apparent molecular mass of the phosphorylated-dephosphorylated form of EBNA-2A was approximately 4 kDa, which is in good agreement with the value of 5 kDa given by Wang et al. (48). It is still an open question whether EBNA-2A undergoes secondary modifications other than phosphorylation; this problem will have to be addressed in future experiments.

Finally, the state of oligomerization of EBNA-2A was analyzed by sucrose gradient centrifugation. Our experiments demonstrated the presence of two forms of EBNA-2A sedimenting at approximately 13S and 34S, much higher values than would be expected for a noncomplexed, monomeric molecule. The observed complexes could represent monomers of EBNA-2A associated with different viral and/or cellular proteins. Alternatively, EBNA-2A might self-associate to dimeric or higher-order complexes in analogy to SV40 large T antigen, which in turn could form complexes with other proteins. We point out, however, that we have no direct experimental evidence of homogeneous complexes of EBNA-2A like dimers or tetramers.

It should be noted that both SV40 large T antigen and EBNA-2A are proteins rich in proline with unusual properties in respect to their behavior on SDS-polyacrylamide gels. They both do not migrate according to their calculated molecular weights, and they both change their electrophoretic mobilities after dephosphorylation (this report and reference 13a). Also, SV40 large T antigen is associated with at least two cellular genes, p53 and the gene product p105 of the retinoblastoma gene locus (7, 23). An association with a host protein(s) might also contribute to the properties of the protein on sucrose gradients. The association of EBNA-2A with two unknown, perhaps cellular, proteins of 37 and 17 kDa has recently been reported (9). When we analyzed EBNA-2A under nonreducing conditions, we indeed observed several bands of EBNA-2A with a low electrophoretic mobilities which might consist of EBNA-2A molecules associated with various unknown proteins. We have not attempted to assay the different fractions of EBNA-2A isolated from the sucrose gradients, since we observed a high background of coprecipitating proteins when we immunoprecipitated ^{35}S-labeled EBNA-2A. Additional experiments will be necessary to clarify the composition of the two complexes of EBNA-2A. Furthermore, detailed studies will

be carried out to determine the state of phosphorylation of the two complexes of EBNA-2A observed on sucrose gradients.

A drastic difference in the mobility of EBNA-2A during SDS-PAGE was observed when the protein was assayed under reducing or nonreducing conditions. A similar phenomenon has recently been described for the terminal protein of EBV, which exhibited a change in electrophoretic mobility depending on the reducing or nonreducing conditions during electrophoresis. The failure to form higher-order complexes under reducing conditions was assumed to result from destruction of disulfide bonds, intra- or intermolecularly, by the reducing agent (13).

ACKNOWLEDGMENTS

This study was supported by the Deutsche Forschungsgemeinschaft grant Mu452/2-2.

We thank G. Brandner (Freiburg, Germany) for making the cell line C57/SV available to us for experiments carried out in his laboratory. We also thank D. Eick (Munich, Germany) for the gift of anti-*myc* antibody.

REFERENCES

1. **Aman, P., M. Rowe, C. Kai, J. Finke, L. Rymo, and G. Klein.** 1990. Effect of the EBNA-2 gene on the surface antigen phenotype of transfected EBV-negative B-lymphoma lines. Int. J. Cancer **45**:77–82.
2. **Billaud, M., P. Busson, D. Huang, N. Mueller-Lantzsch, G. Rousselet, O. Pavlish, H. Wakasugi, J. M. Seigneurin, T. Tursz, and G. M. Lenoir.** 1989. Epstein-Barr virus (EBV)-containing nasopharyngeal carcinoma cells express the B-cell activation antigen Blast2/CD23 and low levels of the EBV receptor CR2. J. Virol. **63**:4121–4128.
3. **Bornkamm, G., J. Hudewentz, U. K. Freese, and U. Zimber.** 1982. Deletion of the nontransforming Epstein-Barr virus strain P3HR-1 causes fusion of the large internal repeat to the DS_L region. J. Virol. **43**:952–968.
4. **Cordier, M., A. Calender, M. Billaud, U. Zimber, G. Rousselet, O. Pavlish, J. Bancherau, T. Tursz, G. Bornkamm, and G. M. Lenoir.** 1990. Stable transfection of Epstein-Barr virus (EBV) nuclear antigen 2 in lymphoma cells containing the EBV P3HR1 genome induces expression of B-cell activation molecules CD21 and CD23. J. Virol. **64**:1002–1013.
5. **Crawford, D. H., M. A. Epstein, G. W. Bornkamm, B. G. Achong, S. Finerty, and J. Thompson.** 1979. Biological and biochemical observations on isolates of EB virus from the malignant epithelial cells of two nasopharyngeal carcinomas. Int. J. Cancer **24**:294–302.
6. **Dambaugh, T., K. Hennessy, S. Fennewald, and E. Kieff.** 1986. The EBV genome and its expression in latent infection, p. 13–45 *In* M. A. Epstein and B. G. Achong (ed.), The Epstein-Barr virus: recent advances. William Heinemann Medical Books Ltd., London.
7. **DeCaprio, J. A., J. W. Ludlow, J. Figge, J. Y. Shew, C. M. Huang, W. H. Lee, E. Marsilio, E. Paucha, and D. M. Livingston.** 1988. SV40 large T antigen forms a specific complex with the product of the retinoblastoma susceptibility gene. Cell **54**:275–283.
8. **Delius, H., and G. W. Bornkamm.** 1978. Heterogeneity of Epstein-Barr virus. III. Comparison of a transforming and a nontransforming virus by partial denaturation mapping of their DNAs. J. Virol. **27**:81–89.
9. **Dillner, J., V. Wendel-Hansen, G. Kjellström, B. Kallin, and A. Rosen.** 1988. Purification and characterization of the Epstein-Barr virus nuclear antigen 2 using monoclonal antipeptide antibodies. Int. J. Cancer **42**:721–727.
10. **Epstein, M. A., and B. G. Achong (ed.).** 1979. The Epstein-Barr virus. Springer-Verlag KG, Berlin.
11. **Fanning, E., B. Nowak, and C. Burger.** 1981. Detection and characterization of multiple forms of simian virus 40 large T antigen. J. Virol. **37**:92–102.
12. **Fennewald, S., V. van Santen, and E. Kieff.** 1984. Nucleotide sequence of an mRNA transcribed in latent growth-transforming virus infection indicates that it may encode a membrane protein. J. Virol. **51**:411–419.
13. **Frech, B., U. Zimber-Strobl, K.-O. Suentzenich, O. Pavlish, G. M. Lenoir, G. W. Bornkamm, and N. Mueller-Lantzsch.** 1990. Identification of Epstein-Barr virus terminal protein 1 (TP1) in extracts of four lymphoid cell lines, expression in insect cells, and detection of antibodies in human sera. J. Virol. **64**:2759–2767.

13a. **Grässer, F., and G. Walter.** Unpublished data.

14. **Grässer, F. A., K. Mann, and G. Walter.** 1987. Removal of serine phosphates from simian virus 40 large T antigen increases its ability to stimulate DNA replication in vitro but has no effect on ATPase and DNA binding. J. Virol. **61**:3373–3380.
15. **Grässer, F. A., K. H. Scheidtmann, P. Tuazon, J. A. Traugh, and G. Walter.** 1988. *In vitro* phosphorylation of SV40 large T antigen. Virology **165**:13–22.
16. **Hammerschmidt, W., and B. Sugden.** 1989. Genetic analysis of immortalizing functions of Epstein-Barr virus in human lymphocytes. Nature (London) **340**:393–397.
17. **Hennessy, K., S. Fennewald, M. Hummel, T. Cole, and E. Kieff.** 1984. A membrane protein encoded by Epstein-Barr virus in latent growth transforming infection Proc. Natl. Acad. Sci. USA **81**:7207–7211.
18. **Herbst, H., G. Niedobitek, M. Kneba, M. Hummel, T. Finn, I. Anagnostopoulos, M. Bergholz, G. Krieger, and H. Stein.** 1990. High incidence of Epstein-Barr virus genomes in Hodgkin's desease. Am. J. Pathol. **137**:13–18.
19. **Hinuma, Y., M. Konn, J. Yamaguchi, D. J. Wudarski, J. R. Blakeslee, Jr., and J. T. Grace, Jr.** 1967. Immunofluorescence and herpes-type virus particles in the P3HR-1 Burkitt lymphoma cell line. J. Virol. **1**:1045–1051.
20. **Jones, C. H., S. D. Hayward, and D. R. Rawlins.** 1989. Interaction of the lymphocyte-derived Epstein-Barr virus nuclear antigen EBNA-1 with its DNA-binding sites. J. Virol. **63**:101–110.
21. **Klein, G.** 1989. Viral latency and transformation: the strategy of Epstein-Barr virus. Cell **58**:5–8.

21a. **Knowles, B.** Personal communication.

22. **Knutson, J. C.** 1990. The level of c-*fgr* RNA is increased by EBNA-2, an Epstein-Barr virus gene required for B-cell immortalization. J. Virol. **64**:2530–2536.
23. **Lane, D. P., and L. V. Crawford.** 1979. T-antigen is bound to a host protein in SV40 transformed cells. Nature (London) **227**: 261–263.
24. **Laux, G., M. Perricaudet, and P. J. Farrell.** 1988. A spliced Epstein-Barr virus gene expressed in immortalized lymphocytes is created by circularization of the linear viral genome. EMBO J. **7**:769–774.
25. **Lenoir, G. M., M. Vuillaume, and C. Bonnardel.** 1985. The use of lymphomatous and lymphoblastoid cell lines in the study of Burkitt's lymphoma, p. 309–318. *In* G. M. Lenoir, G. O'Connor, and C. M. Olwendy (ed.), Burkitt's lymphoma: a human cancer model. IARC scientific series no. 60. Oxford University Press, Oxford.
26. **Lüscher, B., and R. N. Eisenman.** 1988. c-*myc* and c-*myb* protein degradation: effect of metabolic inhibitors and heat shock. Mol. Cell. Biol. **8**:2504–2512.
27. **Mann, K. P., D. Staunton, and D. A. Thorley-Lawson.** 1985. Epstein-Barr virus-encoded protein found in plasma membranes of transformed cells. J. Virol. **55**:710–720.
28. **Miller, G.** 1990. Epstein-Barr virus: biology, pathogenesis, and medical aspects, p. 1921–1958. *In* B. N. Fields et al. (ed.), Virology, 2nd ed. Raven Press, New York.
29. **Mueller-Lantzsch, N., G. M. Lenoir, M. Sauter, K. Takaki, J.-M. Bechet, C. Kuklik-Roos, D. Wunderlich, and G. W. Bornkamm.** 1985. Identification of the coding region for a second Epstein-Barr virus nuclear antigen (EBNA 2) by transfection of cloned DNA fragments. EMBO J. **4**:1805–1811.
30. **Petti, L., C. Sample, and E. Kieff.** 1989. Subnuclear localization and phosphorylation of Epstein-Barr virus latent infection nuclear proteins. Virology **176**:563–574.
31. **Polack, A., G. Hartl, U. Zimber, K.-U. Freese, G. Laux, K.**

Takadi, B. Hohn, L. Gissmann, and G. W. Bornkamm. 1984. A complete set of overlapping cosmid clones of M-ABA virus derived from a nasopharyngeal carcinoma and its similarity to other Epstein-Barr virus isolates. Gene **27**:279–288.

32. **Prives, C.** 1990. The replication functions of SV40 T antigen are regulated by phosphorylation. Cell **61**:735–738.
33. **Pulvertaft, R. J. V.** 1965. A study of malignant tumors in Nigeria by short term tissue culture. J. Clin. Pathol. **18**:261–273.
34. **Raab-Traub, N., R. Pritchett, and E. Kieff.** 1978. DNA of Epstein-Barr virus. III. Identification of restriction enzyme fragments that contain DNA sequences which differ among strains of Epstein-Barr virus. J. Virol. **27**:388–398.
35. **Rabson, M., L. Gradoville, D. R. Rawlins, G. Milman, and G. S. Hayward.** 1985. Sequence specific DNA binding of the Epstein-Barr virus nuclear antigen (EBNA-1) to clustered sites in the plasmid maintenance region. Cell **42**:859–868.
36. **Roeckel, D., and N. Mueller-Lantzsch.** 1985. Biochemical characterization of two Epstein-Barr virus early antigen-associated phosphopolypeptides. Virology **147**:253–263.
37. **Sample, J., D. Liebowitz, and E. Kieff.** 1989. Two related Epstein-Barr virus membrane proteins are encoded by separate genes J. Virol. **63**:933–937.
38. **Sauter, M., H. Boos, F. Hirsch, and N. Mueller-Lantzsch.** 1988. Characterization of a latent protein encoded by the large internal repeats and the BamHI Y fragment of the Epstein-Barr virus (EBV) genome. Virology **166**:586–590.
39. **Sauter, M., and N. Mueller-Lantzsch.** 1987. Characterization of an Epstein-Barr virus nuclear antigen 2 variant (EBNA2B) by specific sera. Virus Res. **8**:141–152.
40. **Scheidtmann, K.** 1986. Phosphorylation of simian virus 40 large T antigen: cytoplasmatic and nuclear phosphorylation sites differ in their metabolic stability. Virology **150**:85–95.
41. **Scheidtmann, K.-H., M. Hardung, B. Echle, and G. Walter.** 1984. DNA-binding activity of simian virus 40 large T antigen correlates with a distinct phosphorylation site. J. Virol. **50**:1–12.
42. **Schickedanz, J., K. H. Scheidtmann, and G. Walter.** 1986. Kinetics of nuclear transport and oligomerization of simian virus 40 large T antigen. Virology **148**:47–57.
43. **Schöffel, A., S. Weist, R. K. Ball, K.-H. Scheidtmann, D. G. Braun, and G. Brandner.** 1988. Synthetic oligopeptides define epitopes at the amino- and carboxy-terminus of simian virus 40 large tumor antigen which are recognized by monoclonal antibodies. Virology **166**:245–247.
44. **Sugden, B.** 1989. An intricate route to immortality. Cell **57**:5–7.
45. **Wang, D., D. Liebowitz, and E. Kieff.** 1985. An EBV membrane protein expressed in immortalized lymphocytes transforms established rodent cell lines. Cell **43**:831–840.
46. **Wang, F., C. Gregory, C. Sample, M. Rowe, D. Liebowitz, R. Murray, A. Rickinson, and E. Kieff.** 1990. Epstein-Barr virus latent membrane protein (LMP1) and nuclear proteins 2 and 3C are effectors of phenotypic changes in B lymphocytes: EBNA-2 and LMP1 cooperatively induce CD23. J. Virol. **64**:2309–2318.
47. **Wang, F., C. D. Gregory, M. Rowe, A. B. Rickinson, D. Wang, M. Birkenbach, H. Kikutani, T. Kishimoto, and E. Kieff.** 1987. Epstein-Barr virus nuclear antigen 2 specifically induces expression of the B-cell activation antigen CD23. Proc. Natl. Acad. Sci. USA **84**:3452–3456.
48. **Wang, F., L. Petti, D. Braun, S. Seung, and E. Kieff.** 1987. A bicistronic Epstein-Barr virus mRNA encodes two nuclear proteins in latently infected, growth-transformed lymphocytes. J. Virol. **61**:945–954.
49. **Wang, F., S. F. Tsang, M. G. Kurilla, J. I. Cohen, and E. Kieff.** 1990. Epstein-Barr virus nuclear antigen 2 transactivates latent membrane protein LMP1. J. Virol. **64**:3407–3416.